Intrinsic and Heat-Induced Exchange Coupling through Amorphous Silicon

B. Briner and M. Landolt
Laboratorium für Festkörperphysik, Eidgenössische Technische Hochschule Zürich, CH-8093 Zürich, Switzerland
(Received 18 August 1993; revised manuscript received 18 November 1993)

We show that ferromagnetic films separated by a spacer of amorphous Si are exchange coupled for Si thicknesses $d_{Si} \leq 40$ Å. For 14 Å $< d_{Si} <$ 22 Å we observe antiferromagnetic coupling. The coupling strength of approximately 5×10^{-6} J/m^2 is strongly temperature dependent with a positive temperature coefficient. We suggest that localized electronic defect states in the gap of amorphous Si mediate the exchange interaction. The particular coupling mechanism encountered here also works with noncrystalline ferromagnetic layers.

PACS numbers: 75.30.Et, 75.70.Fr, 78.66.Sq

The discovery of oscillatory exchange coupling in magnetic multilayers [1] and the subsequent observation that this phenomenon exists for a wide variety of transition- and noble-metal spacer materials [2] have provoked a true renaissance of both theoretical and experimental research in magnetism. The mechanisms thought to be responsible for the coupling phenomena [3] all rely on two main properties of the spacer material: its metallic character and crystalline orientation. One might thus be lead to the conclusion that both are necessary requirements for the existence of exchange coupling in layered systems. However, we have shown that exchange coupling multilayers also exists for a different class of spacer materials: amorphous semiconductors [4] and insulators [5]. In this Letter we report a pronounced temperature dependence of the exchange coupling through amorphous Si. The observed positive temperature coefficient gives clear evidence of semiconducting spacer behavior. New measurements on Fe/a-Si/Fe trilayers confirm that ferromagnetic (FM) as well as antiferromagnetic (AFM) coupling occurs depending on the thickness of the Si layer. Over the entire thickness range up to 40 Å we find only one antiferromagnetic region. AFM-coupled trilayers display a very low coupling strength of 5×10^{-6} J/m^2, which is at least 2 orders of magnitude smaller than the values observed on metallic Fe-silicide multilayers [6]. Thermal activation in general is found to increase the coupling strength in both AFM and FM regions, and in special cases it can even change the sign of the coupling. We wish to strongly emphasize that our earlier observations of light-induced exchange coupling through a-Si [7] as well as a-SiO [8] were based on an incorrect temperature determination. Extensive investigations revealed that in the above cases all the changes of the coupling upon light irradiation must indeed be attributed to sample heating by the light source. On the other hand, no light effects can be seen when the samples are kept at constant temperature. This observation clearly is in contrast to the recent report by Mattson *et al.* [9], who have found photosensitive coupling in multilayers with spacers composed of an unknown mixture of Fe silicides.

Based on the observed strong temperature dependence we infer that the coupling mechanism encountered with nonmetallic spacers is different from the one commonly seen in metallic multilayers. We propose that localized electronic states in the gap of the amorphous semiconductor are responsible for mediating magnetic information across the nonmetallic barrier. Direct tunneling or activation of carriers to the conduction band of Si can be ruled out as possible mechanisms for the exchange coupling because these processes display nearly no temperature dependence as soon as the gap energy becomes large compared to kT—a condition which is satisfied in a-Si. The extension of magnetic exchange coupling to multilayers with nonmetallic components opens a new window in the research of magnetism. We feel—to dare a speculative outlook—that the potential to modify magnetic coupling with external parameters such as heat is of quite considerable relevance for future technical applications.

Sample preparation and subsequent magnetic measurements are performed in a UHV chamber with a base pressure of 10^{-10} Torr. A cryostat cooled with liquid He keeps the samples at $T = 40$ K during preparation and experiments. As a substrate we use an amorphous magnetic ribbon, consisting of $Fe_{40}Ni_{40}B_{20}$. This substrate displays a square hysteresis loop with a small coercive field of ~0.5 Oe. It serves as a magnetic driver, because any ferromagnetic film evaporated directly on the ribbon is strongly exchange coupled to the substrate and acquires the same coercive force. The external magnetic field necessary to drive the substrate to saturation is provided by a small horseshoe electromagnet.

Prior to sample growth the substrate is sputter cleaned with Ne^+ ions. Fe and n-type Si (Sb doped) are evaporated by e-beam bombardment, in a pressure less than 10^{-9} Torr. Evaporation rates of about 3 Å/min are controlled with a quartz-crystal thickness monitor. Independently we use Auger electron spectroscopy (AES) to determine the thickness and cleanliness of all evaporated films.

The magnetic measurements are performed with spin-polarized secondary-electron emission (SPSEE). 1 keV electrons impinging on the sample excite a cascade of sec-

0031-9007/94/73(2)/340(4)$06.00

ondary electrons. The low-energy secondaries are emitted with high intensity and—in the case of a ferromagnetic surface—with high spin polarization [10]. For spin analysis the electrons are accelerated to 100 keV and the asymmetry in scattering from a gold foil is determined. The measured polarization $P = (N\uparrow - N\downarrow)/(N\uparrow + N\downarrow)$ is proportional to the magnetization of the sample at the surface. Because of the low energy of the analyzed secondary electrons SPSEE is a very surface-sensitive magnetic probe.

For the present Fe/a-Si/Fe samples we start by growing 15–20 Å of Fe on the $Fe_{40}Ni_{40}B_{20}$ ribbon at $T =$ 300 K. Before Si evaporation the sample is cooled to $T = 40$ K and a reference hysteresis loop is taken. The Si barrier and the topmost Fe layer are evaporated at low temperature to reduce Fe-Si interdiffusion. An AES growth study of Si on Fe shows that under these conditions extended silicide formation does not occur. Considering the limited sensitivity of AES we cannot fully exclude silicide formation in the initial stage of growth. However, the positive temperature coefficient of the exchange coupling provides direct evidence of semiconducting spacer behavior for $d_{Si} > 13$ Å. Thus we can set this thickness as an upper bound of the range where metallic silicides might form. After having finished the trilayer by again evaporating 15–20 Å of Fe we measure a second hysteresis loop, which due to the surface sensitivity of SPSEE shows the magnetic response of only the topmost Fe layer. For the sample depicted in Fig. 1 the inverted hysteresis loop of the Fe overlayer clearly indicates AFM coupling through 18 Å of a-Si. Because of exchange coupling the overlayer hysteresis exhibits the same low coercive field as the substrate. An uncoupled Fe film, on the other hand, does not show any remanence when exposed to the low external magnetic fields used here.

Anisotropies and magnetostatic energies in the uncoupled Fe overlayer are such as to break it up into magnetic domains. As a consequence the Fe overlayer exhibits a linear response of M to a weak magnetic field, regardless of whether this field is established by exchange coupling or applied externally. Therefore we can, as a first step, linearly correlate the polarization at remanence with the coupling strength. Figure 2 gives an overview of how the polarization at remanence changes with Si thickness. Three different sets of data are compared. The data exhibit some scatter which reflects different growth modes, but, as a remarkable result, they all divide in three regions. For a-Si thicknesses below 13 Å, denoted as region I, we find FM coupling. In an intermediate thickness range between 14 and 22 Å, denoted as II in Fig. 2, the coupling is predominantly AFM or near zero for some species. At about 22 Å the coupling again switches sign and stays ferromagnetic for thicknesses up to 40 Å (region III). In data set 1 (from Ref. [4]) the first Fe layer adjacent to the substrate is grown at 40 K, whereas in set 2 (present work) it is evaporated at room temperature. We find that growing the first Fe layer at room temperature allows us to observe exchange coupling up to at least 40 Å, probably due to a better surface quality of the first Fe film.

To test the possible influence of Fe-Si diffusion on the coupling phenomenon we have decided to alternatively grow the a-Si barrier directly on the $Fe_{40}Ni_{40}B_{20}$ substrate without prior Fe evaporation. We observe that FeNiB/a-Si/Fe samples are always more stable against irreversible thermally induced changes than Fe/a-Si/Fe samples, in

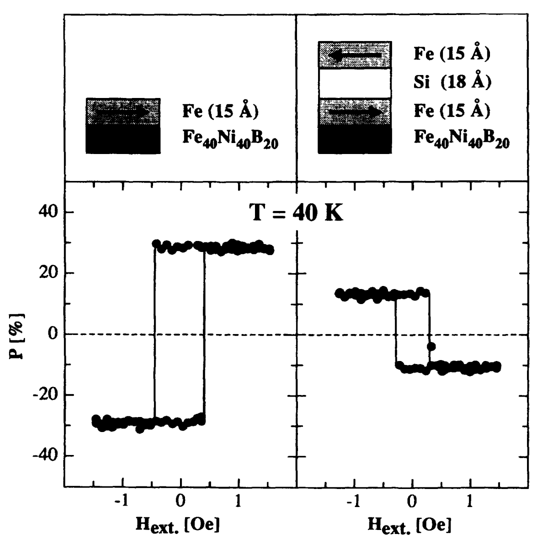

FIG. 1. SPSEE hystereses of the first Fe layer coupled to the substrate (left panel) and of the Fe cover layer of the Fe/Si (18 Å)/Fe sandwich (right panel), showing AFM coupling through 18 Å of amorphous Si.

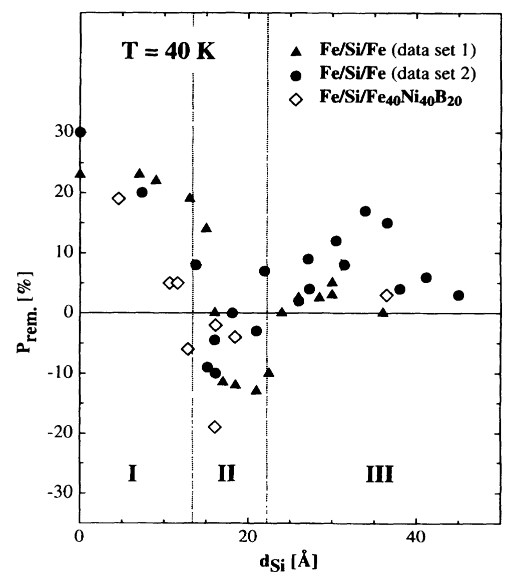

FIG. 2. Spin polarization of secondary electrons, i.e., top-layer magnetization at remanence versus Si thickness of Fe/Si/Fe and FeNiB/Si/Fe trilayers. Three different regions of exchange coupling are distinguished.

line with the fact that the amorphous structure of the substrate due to the lack of grain boundaries inhibits diffusion of Fe or Ni into the silicon layer [11]. Because we cannot evaporate an amorphous ferromagnetic alloy we again finish the structures with a 15 Å thick Fe film. The results obtained with the FeNiB/Si/Fe samples are included in Fig. 2. Again we find the same three coupling regions, and AFM coupling is observed in the same Si-thickness range as with Fe/Si/Fe. This confirms the fact that the observed exchange coupling is an intrinsic quality of the a-Si barrier. Some difference from the Fe/Si/Fe trilayers occurs in region I. The samples without the first Fe film display weaker FM coupling. We attribute this difference to the reduced diffusion at the first interface when going from pure Fe to the amorphous alloy. This allows us to create smaller Si barriers without possible exchange coupling through diffusion-generated ferromagnetic bridges. The results on FeNiB/Si/Fe samples furthermore show that the particular coupling mechanism encountered here does not require the ferromagnetic layers to be crystalline. This is a remarkable result also with respect to future applications where the use of ferromagnetic alloys for thermal stabilization of the interfaces can become very important.

We have not succeeded in producing AFM coupling with Si spacer layers grown at room temperature. Thus we believe that keeping the sample at $T = 40$ K during Si evaporation is essential either to provoke a large defect density in the spacer material or to inhibit surface diffusion. We find, on the other hand, that after completed growth we can slightly heat the trilayers without introducing irreversible structural changes. They only occur for temperatures above ≈ 200 K and must be attributed either to the reduction of defect states by annealing or to interdiffusion.

Next we address the magnitude of the coupling strength. On AFM-coupled trilayers we can directly measure the strength of the exchange coupling simply by increasing the external magnetic field up to the point where it compensates the negative exchange field. As shown in Fig. 3 we typically find compensation fields of $H_{\text{comp}} = 15$ Oe, corresponding to coupling strengths of 5×10^{-6} J/m^2 [12]. These values are very low, if compared to the fields of some kOe necessary to align AFM-coupled metallic multilayers [6]. Figure 3 also illustrates the pronounced temperature dependence of the exchange coupling. At $T = 150$ K the external field needed to depolarize the Fe overlayer is about twice as large as at $T = 40$ K. We want to emphasize that the increase in H_{comp} is accompanied by a corresponding increase of the overlayer polarization at remanence. This nicely demonstrates the correlation of P_{rem} with the coupling strength.

The positive temperature coefficient of the exchange coupling provides clear evidence for semiconducting

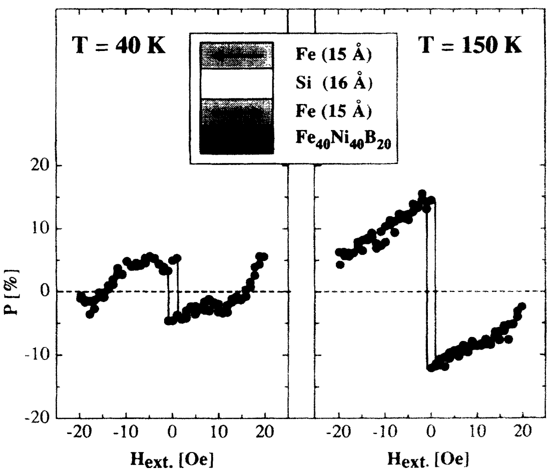

FIG. 3. SPSEE hystereses of AFM coupled Fe/Si (16 Å)/Fe trilayers at $T = 40$ K (left panel) and 150 K (right panel), respectively. At $T = 40$ K the exchange field is compensated with $H_{\text{comp}} = 15$ Oe. At $T = 150$ K the coupling strength is about twice as large as at 40 K.

spacer behavior and directly corresponds to the observations on Fe/a-SiO/Fe trilayers [5]. To precisely determine the temperature of the sample area under investigation we use a 0.05 mm diam. chromel-alumel thermocouple which is attached to the back side of the very thin metglass substrate with silver paint. Sapphire spacers ensure thermal contact with the cooling head of the cryostat. A small Ta filament which is also mounted in the back of the substrate delivers the radative power necessary to heat the sample from 40 to 300 K in less than 1 min. The possibility to quickly change the temperature allows us to reversibly observe the temperature dependence of the exchange coupling even in samples which are in a metastable state and gradually change their structure due to annealing of diffusion.

Figure 4 shows the temperature dependences of the exchange coupling for two samples with $d_{\text{Si}} = 15$ and 45 Å, respectively. The sample with the thinner Si barrier is weakly AFM coupled at $T = 40$ K. Heating to 150 K strongly increases the AFM coupling. The trilayer with $d_{\text{Si}} = 45$ Å, on the other hand, displays nearly no coupling at low temperature, but thermal activation induces considerable FM coupling at $T = 250$ K. In both cases the dots and open circles represent two successive heating runs and thus illustrate the reversibility of the observation. We note that thermally induced ferromagnetic coupling occurs even for Si barriers as thick as 60 Å where exchange at $T = 40$ K is below the detection limit. The examples given in Fig. 4 are representative in the sense that heat input generally leads to an increase of the coupling strength regardless of its sign. However, we have also found an exception to this general trend. A sample with a 22 Å thick a-Si spacer exhibits weak FM coupling at $T = 40$ K. Heating this

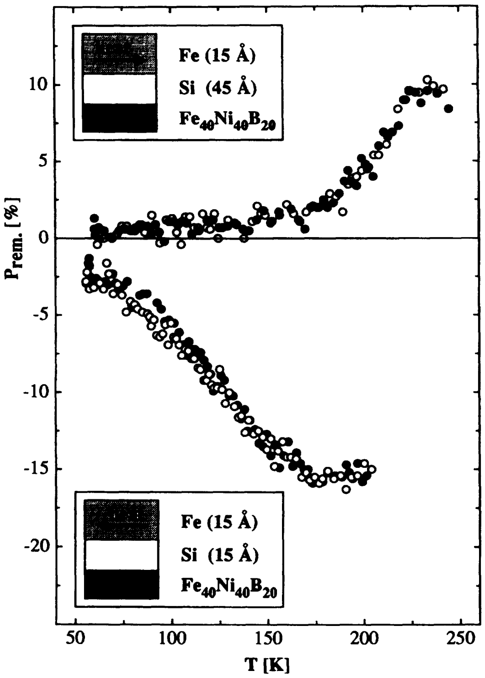

FIG. 4. Spin polarization of secondary electrons, i.e., toplayer magnetization at remanence versus temperature. Top: thermally induced FM coupling across 45 Å of a-Si. Bottom: At $d_{Si} = 15$ Å, AFM coupling is thermally induced. Dots and open circles represent two successive heating cycles.

sample to about $T = 250$ K reversibly leads to a sign change of the coupling. This observation has to do with the fact that the barrier thickness lies near the zero-crossing point of the coupling.

As a possible mechanism for mediating magnetic exchange we propose resonant tunneling of polarized electrons through defect-generated localized electronic states in the gap of the nonmetallic barrier. These states are present in all amorphous semiconductors and insulators, and they determine the electrical conductivity in these materials. The resonance energy of a localized defect varies with its occupation state because of the electron-correlation energy. Therefore thermal excitation can repopulate the localized states and thus alter the number of empty or singly occupied resonances available for spin-dependent resonant tunneling. The striking observation that AFM coupling does occur in a-Si but not in a-SiO [5] reflects the strong response of the exchange coupling to changes of the electronic-structure parameters in nonmetallic spacers. For instance, it has been shown [13] that even direct tunneling through a simple rectangular barrier can lead to FM as well as to AFM coupling depending on the barrier height. The questions of how the density of localized states around the Fermi energy as well as the barrier height change with spacer thickness presumably touch the key for understanding the exchange coupling through amorphous nonmetallic materials.

We wish to thank H. C. Siegmann for his continuous support and many fruitful conversations. This work has largely profited from the excellent technical support of K. Brunner and from a pleasant collaboration with U. Ramsperger. P. Reimann, and H. J. Güntherodt, University of Basel, have kindly provided the vacuum-cast FeNiB substrates. Financial support by the Schweizerischer Nationalfonds is gratefully acknowledged.

[1] P. Grünberg, R. Schreiber, Y. Pang, M. N. Brodsky, and H. Sowers, Phys. Rev. Lett. **57**, 2442 (1986).
[2] S. S. P. Parkin, Phys. Rev. Lett. **67**, 3598 (1991).
[3] P. Bruno and C. Chappert, Phys. Rev. B **46**, 261 (1992); J. Mathon, M. Villeret, and D. Edwards, J. Phys. Condens. Matter **4**, 9873 (1992).
[4] S. Toscano, B. Briner, H. Hopster, and M. Landolt, J. Magn. Magn. Mater. **114**, L6 (1992).
[5] S. Toscano, B. Briner, and M. Landolt, in *Magnetism and Structure of Systems in Reduced Dimensions*, edited by R. F. C. Farrow *et al.*, NATO ASI Ser. B, Vol. 309 (Plenum, New York, 1993), p. 257; S. Toscano, dissertation ETH No. 9915, Zürich, 1992.
[6] E. E. Fullerton, J. E. Mattson, S. R. Lee, C. H. Sowers, Y. Y. Huang, G. Felcher, and S. D. Bader, J. Magn. Magn. Mater. **117**, L306 (1992).
[7] B. Briner and M. Landolt (unpublished).
[8] B. Briner and M. Landolt, Z. Phys. B **92**, 137 (1993).
[9] J. E. Mattson, S. Kumar, E. E. Fullerton, S. R. Lee, C. H. Sowers, M. Grimsditch, S. D. Bader, and F. T. Parker, Phys. Rev. Lett. **71**, 185 (1993).
[10] M. Landolt, in *Polarized Electrons in Surface Physics*, edited by R. Feder (World Scientific, Singapore, 1985), p. 385.
[11] K. H. J. Buschow, in *High Density Digital Recording*, edited by K. H. J. Buschow *et al.*, Nato ASI Ser. E, Vol. 229 (Plenum, New York, 1992).
[12] We determine the coupling strength as $J = d_{Fe} M_S H_{comp}$, with $d_{Fe} = 20$ Å, $M_S = 2.2$ T, and $H_{comp} = 15$ Oe.
[13] J. C. Slonczewski, Phys. Rev. B **39**, 6995 (1989).

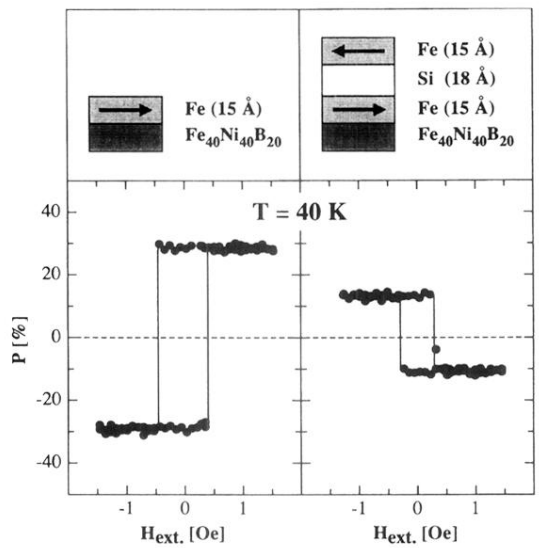

FIG. 1. SPSEE hystereses of the first Fe layer coupled to the substrate (left panel) and of the Fe cover layer of the Fe/Si (18 Å)/Fe sandwich (right panel), showing AFM coupling through 18 Å of amorphous Si.

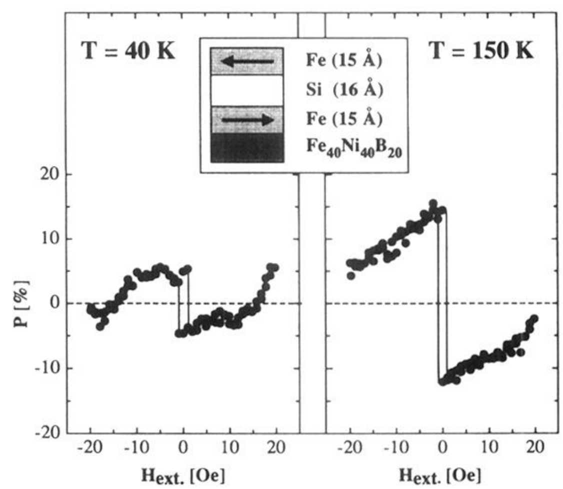

FIG. 3. SPSEE hystereses of AFM coupled Fe/Si (16 Å)/Fe trilayers at $T = 40$ K (left panel) and 150 K (right panel), respectively. At $T = 40$ K the exchange field is compensated with $H_{\mathrm{comp}} = 15$ Oe. At $T = 150$ K the coupling strength is about twice as large as at 40 K.

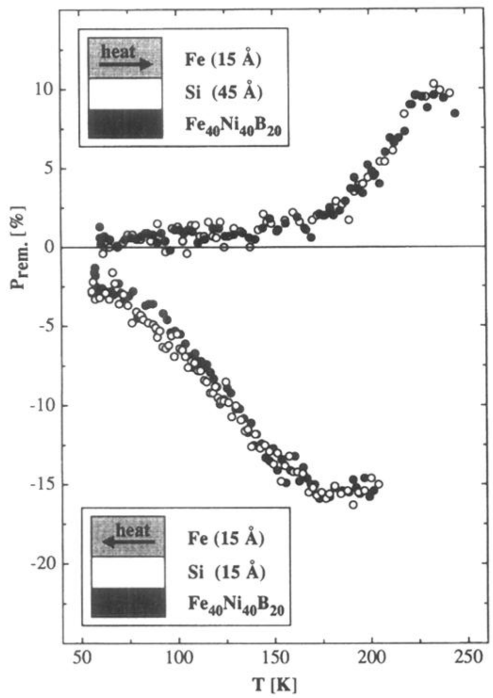

FIG. 4. Spin polarization of secondary electrons, i.e., top-layer magnetization at remanence versus temperature. Top: thermally induced FM coupling across 45 Å of *a*-Si. Bottom: At d_{Si} = 15 Å, AFM coupling is thermally induced. Dots and open circles represent two successive heating cycles.